Siloxane Polymers for High-Resolution, High-Accuracy Soft Lithography

H. Schmid and B. Michel*

IBM Research, Zurich Research Laboratory, 8803 Rüschlikon, Switzerland

Received December 31, 1998; Revised Manuscript Received January 3, 2000

ABSTRACT: We report the formulation of siloxane polymers for high-resolution, high-accuracy stamps for soft lithography. With this technique, a molecular, polymeric, or liquid ink is applied to the surface of a stamp and then transferred by conformal contact to a substrate. Stamps for this technique are usually made of a commercial siloxane elastomer with appropriate mechanical properties to achieve conformal contact but are incapable of printing accurate, submicrometer patterns. To formulate better stamp polymers, we used models of rubber-like elasticity as guidelines. Poly(dimethylsiloxane) networks were prepared from vinyl and hydrosilane end-linked polymers and vinyl and hydrosilane copolymers, with varying mass between cross-links and junction functionality. The polymer formulations were characterized by strain at break as well as compression modulus and surface hardness measurements. This resulted in the identification of bimodal polymer networks having mechanical properties that allow the replication of high-density patterns at the 100 nm scale and that withstand the mechanical constraints during use as a stamp material. We also demonstrate advantageous implementations of the formulated polymers in hybrid stamps that achieve submicrometer-dimensional accuracy over large areas.

1. Introduction

Siloxane-based elastomers have found widespread use as sealants,[1] for encapsulation and packaging of electronic components,[2] in medicine,[3] and, most recently, for soft lithography.[4] In addition to their technological importance, end-linked siloxanes are used as model systems for rubber-like elasticity: By employing end-linking reactions, the number of monomer units between junctions and the functionalities of the junctions can be controlled, allowing a much better interpretation and prediction of physical properties of siloxane rubbers.[5,6] In this paper we use published theories of rubber-like elasticity to predict moduli of siloxane polymers, which are tested for specific application in soft lithography.

Molecular theories of rubber-like elasticity are based on network chains being Gaussian random coils with retractive forces arising from a decrease in entropy as a result of deformation.[7−9] The models predict the modulus or reduced force (F^*) of an elastic material to be inversely proportional to the molecular mass between cross-links (M_c) and, for the phantom model, proportional to the junction functionality ϕ.[10−12] An additional constant c accounts for "affine" deformations in which cross-links move linearly with the macroscopic dimensions of the sample:[12]

$$F^*_{\text{affine}} = cRT\nu^{2/3}M_c^{-1} \qquad (1)$$

where R is the gas constant, T is the temperature (K), and ν is the volume fraction of the cross-linked chains. Phantom models predict smaller moduli than affine models do because the chains can transect one another and the cross-links fluctuate freely:[13,14]

$$F^*_{\text{phantom}} = \chi RT\nu^{2/3} \qquad (2)$$

where the factor χ equals $(1 - 2/\phi)M_c^{-1}$. The closeness with which a real network approaches the affine limit

depends on the firmness with which the cross-links are embedded in the network structure by chain−cross-link entangling. In addition to physical cross-links, molecular entanglements also contribute directly to the small-strain modulus, whereas there is no significant effect on the large-strain modulus.[5] Knowledge of both ϕ and M_c permits a direct estimation of the modulus with good accuracy.[12] Prediction of strain at break or toughness, however, is much more difficult, and no convincing models have been presented in the literature.

Bimodal networks are composed of an end-linked mixture of very short and relatively long chains. Surprisingly, such short links do not constitute the "weakest" links but provide greater strength and toughness. Bimodal networks can be spatially as well as compositionally heterogeneous, e.g., with short, randomly distributed links, with heavily cross-linked clusters joined to long chains, or with inorganic fillers.[12] Bimodal networks created by filling with organic or inorganic nanoparticles require homogeneous dispersion and good polymer−filler interaction to achieve superior mechanical properties.[12,15,16]

Soft lithography[4] relies on a stamp to bring a reactant in contact with a substrate. Stamps are typically replicated by molding and curing a liquid prepolymer from a master of photoresist, silicon, or metal. Stamp materials in soft lithography are subjected to capillary forces, self-adhesion, and mechanical stresses during printing. These stresses before or during printing can deform the stamp or cause parts of it to collapse, which leads to defective and inaccurate prints. Most of the work on contact printing has been done using Sylgard 184 (Dow Corning, Midland), a commercially available thermocured siloxane polymer, whose structures smaller than 1 μm tend to merge or collapse during inking and printing.[17] Previous studies of collapse as a function of curing time suggest that the goal to print smaller features in accurate layouts is best accomplished with a stamp polymer having a higher modulus and greater surface hardness. Too high a modulus and too great a surface hardness, however, lead to brittle materials that can no longer adapt and conform to a substrate.

---

* To whom correspondence should be addressed. E-mail: bmi@zurich.ibm.com.

Table 1. New Blends Prepared Using Different Vinyl and Hydrosilane Prepolymers

Vinyl-Terminated Polydimethylsiloxanes and Vinylmethylsiloxane−Dimethylsiloxane Copolymers

M_c (D)	MW (D)	%	name
550	550	11	DMS-V03
770	770	7.9	DMS-V05
6000	6000	1.0	DMS-V21
9400	9400	0.5	DMS-V22
17200	17200	0.4	DMS-V25
28000	28000	0.22	DMS-V31
49500	49500	0.12	DMS-V35
7400	~30000	1	VDT-131
1644	~30000	4.5	VDT-431
987	~30000	7.5	VDT-731
512	>20000	12	VDT-954
<100	~1000	100	VMM-010

Methylhydrosilane−Dimethylsiloxane Copolymers

ϕ	MW (D)	%	name
2	1950	6.5	HMS-071
4.3	1950	16.5	HMS-151
7.2	1950	27.5	HMS-301
7.4	1050	52.5	HMS-501
23	1950	100	HMS-991/PS-120

The diverging demands on conformality, high pattern stability, small thermal or mechanical expansion, and runout cannot be met by one material alone but require layered structures.[18] A practical method to compensate partially for insufficient dimensional and mechanical stability of polymeric materials is to mold the stamp polymer on top of a rigid glass backplane.[19] Such hybrid stamps have better overall accuracy,[20] but stresses generated upon cooling of the polymer layer cast against rigid supports account for small nonuniform distortions. Very thin polymer layers (<0.1 mm) appear to solve this problem but are exposed to homogeneously distributed stresses.[21] These stamps have a limited ability to compensate for substrate topography, however, and are useful only for lithography applications on flat substrates.[19] We report the formulation of appropriate polymers and their use in a technological implementation, and show that changes in the network parameters directly affect the performance of the final product, the hybrid stamp. Changes in the design of the supporting backplane recursively require changes in the network parameters of the polymers. The design of optimal

stamps for soft lithography is an effort involving polymer chemistry, surface science, and technology.

2. Materials and Methods

2.1. Network Formation. Sylgard 184 provided the reference material for our comparative materials studies. New blends were prepared using different vinyl and hydrosilane prepolymers (ABCR, Germany); see Table 1. Prepolymers were used as received from ABCR without further purification. Preparation of polymers typically required the addition of 5 ppm w/w platinum catalyst to the vinyl fraction (platinum−divinyltetramethyldisiloxane complex in xylene (SIP 6831.1, ABCR, Germany) and of 0.1% w/w modulator to the mixture (2,4,6,8-tetramethyltetravinylcyclotetrasiloxane, Fluka, Switzerland) as indicated in Table 2.

The catalyst and modulator were added to the vinyl compound prior to the hydrosilane component and then mixed carefully. The mixture was left until trapped air bubbles had escaped and then poured into glass dishes for surface hardness measurements, or injected into molds for compression modulus measurements, Young's modulus, and strain-at-break experiments. Samples were cured for 24 h at 60 °C unless noted otherwise. Filler materials such as hexamethyldisilazane-treated silica (SI6962.0, ABCR, Germany) and a specialty vinyl-modified polymer (VQM-135, ABCR, Germany) were worked into the vinyl component prior to mixing in the hydrosilane component.

Model PDMS networks require formulations with a stoichiometric reaction among vinyl end-functionalized prepolymers and hydrosilane linkers. Two temperature-dependent side reactions change the effective concentration of the reactive groups[22] and require an optimization of the stoichiometric ratios to allow determination of the effective junction functionality. Studying all the materials with at least three different hydrogen-to-vinyl ratios was therefore particularly important. Typically the best polymers were formed at hydrogen-to-vinyl ratios of 1.5:1, although this varied considerably (between 1.1 and 3:1).[22] Surface-hardness samples were made and measured for almost all material mixtures. Samples for compression modulus, Young's modulus, and strain-at-break measurements were more difficult to make because they require molding and demolding. Samples with trapped gas bubbles and very soft samples could not be demolded without being disrupted and, therefore, did not allow measurement of these parameters. Failure is indicated by "foam" and "too soft" in Table 2.

2.2. Mechanical Measurements. Standard surface-hardness tools[23] fail to yield consistent results over the entire scope of materials studied. This triggered the development of a different method to determine surface hardness: Shore A and

Table 2. Surface Hardness as a Function of Vinyl Ratio in the Prepolymer and Hydrosilane Ratio in the Cross-Linker[a]

%	wt % vinyl in prepolymer	M_c	surface hardness % of glass, H-to-vinyl ratio 1.25	1.5	2	compression modulus (N mm^{-2})	elong at break
wt % hydrosilane in	12	512	0.41	**0.44**	0.31	1.64 ± 0.03	8.6
cross-linker 6.5,	7.5	987	**0.51**	0.43	0.30	2.12 ± 0.12	6.7
$\phi = 2$, $M_{c_2} = 1950$ D	4.5	1644	**0.56**	0.40	0.30	1.81 ± 0.05	7.5
	1.0	7400	**0.16**	0.15	0.11	too soft	13.6
wt % hydrosilane in	12	512	**2.23**	1.61	1.89	7.81 ± 0.52	9.3
cross-linker 16.5,	7.5	987	**1.78**	1.43	1.00	3.91 ± 0.06	10.7
$\phi = 4.3$, $M_{c_2} = 1950$ D	4.5	1644	**1.00**	0.94	0.72	4.21 ± 0.06	10.1
	1.0	7400	0.22	**0.24**	0.2	0.60 ± 0.02	20.0
wt % hydrosilane in	12*	512	**2.04**	1.42	1.18	foam	foam
cross-linker 27.5,	7.5*	987	**2.59**	2.10	1.43	**8.97 ± 0.21**	**5.7**
$\phi = 7.2$, $M_{c_2} = 1950$ D	4.5	1644	1.51	**1.52**	1.24	6.51 ± 0.14	7.2
	1.0	7400	0.26	**0.28**	0.24	0.79 ± 0.02	18.4
wt % hydrosilane in	12*	512	foam	foam	foam	foam	foam
cross-linker 52.5,	7.5*	987	2.02	**2.77**	1.61	8.57 ± 0.12	8.7
$\phi = 7.4$, $M_{c_2} = 1050$ D	4.5	1644	1.15	**1.75**	1.40	4.67 ± 0.32	11.7
	1.0	7400	0.21	0.29	**0.31**	0.73 ± 0.07	28.4

[a] Three different mixtures with hydrosilane-to-vinyl ratios of 1.25, 1.5, and 2 have been prepared for each sample. The compression modulus and elongation at break were measured for the mixtures with the greatest surface hardness (bold). The values of the overall optimal polymer (material A) are underlined. (asterisks indicate 0.1% modulator added).

Shore D measurements always induce defects in the measured area and are not surface-sensitive enough to characterize thin layers. We determined the resistance of a surface to penetration by a hard sphere with a diameter of 1 mm and compared it to the resistance of a glass surface.[24] To improve the accuracy of our measurements, we recorded the entire force-versus-distance (10 mg resolution, 1 μm step size) curve on an analytical balance, which also allowed detection of the sudden failure of thin surface layers and of contamination-inhibited curing at surfaces. Typically, standard deviations of three subsequent measurements of the same area were compared to those of three different areas to allow an estimation of the long-range homogeneity of the material and curing process.

Compression moduli were measured on molded posts (4 mm in diameter, 10 mm long) compressed on a balance using a matching metal post mounted on a stiff stepper-motor-controlled drive. Material homogeneities were checked using force-versus-distance profiles and by averaging over several posts. Young's modulus and elongation at break were determined using "dog bones" with cross sections of 4 × 4 and 2 × 2 mm². Work of adhesion[25] was measured by acquiring force-versus-distance profiles of a 4 mm diameter post pressed onto a gold-covered silicon wafer up to a maximal force of 2 g and withdrawn by the same distance. The work of adhesion was calculated by taking the difference between loading and unloading integrals.

2.3. Master Fabrication and Molding. Masters with structures larger than 1 μm were fabricated by contact photolithography on silicon wafers. High-resolution masters for molding were fabricated from silicon-on-insulator (SOI) wafers. Electron-beam lithography was used to expose the photoresist-coated wafers. After development of the resist, the pattern was transferred through the silicon to the oxide layer of the wafer, resulting in structures having well-defined corners at the bottom. This method prevented deterioration of the stamp geometry. Stamps were molded after coating with a 5 nm thick, plasma-deposited, fluorinated separation layer (STS, Bristol, U.K.) and released from the master at the curing temperature to avoid a buildup of tension due to thermal shrinkage. Stamps were investigated for structural stability and integrity in a scanning electron microscope (SEM) immediately after demolding and again after several inking and printing cycles. Reliable imaging required a sputter coating with 10 nm of Au onto the polymer surface.

2.4. Metrology. Long-range distortions of the patterns were measured on a calibrated *XY*-stage with 1 μm accuracy (Leitz, WM digital with modified optics) by comparing two prints of the same stamp with each other and with the master. The *X* and *Y* coordinates of 20 reference points on a 50 mm circumference were recorded on the chromium master, the stamp, and the prints. By cutting the patterned substrates in stripes and aligning corresponding parts, relative measurements with submicrometer resolution were taken using a high-resolution optical microscope. Overlay accuracy tests were performed on a modified mask aligner (MA 420, EVI Schaerding) by measuring the registry of alignment marks with those on a previously printed pattern using the split-field microscope of this instrument. This measurement allowed overlay errors to be assessed down to the resolution limit of the instrument (approximately 1 μm) over an area of 50 mm².

3. Results

Sylgard 184 is formulated from a vinyl-terminated prepolymer linked via a short hydrosilane cross-linker using a platinum complex as catalyst. Curing times of 24 h and a curing temperature of 60 °C at a recommended mixing ratio of 10:1 (w/w resin to cross-linker) produced a material with a compression modulus of 2 N/mm², a surface hardness of 0.7% of glass (65 ± 1 Shore A), and strain at break of approximately 50%. Moduli of the elastomers cured under the above conditions can vary up to 15% depending on the mixing method, catalyst, and modulator concentration.[23,26]
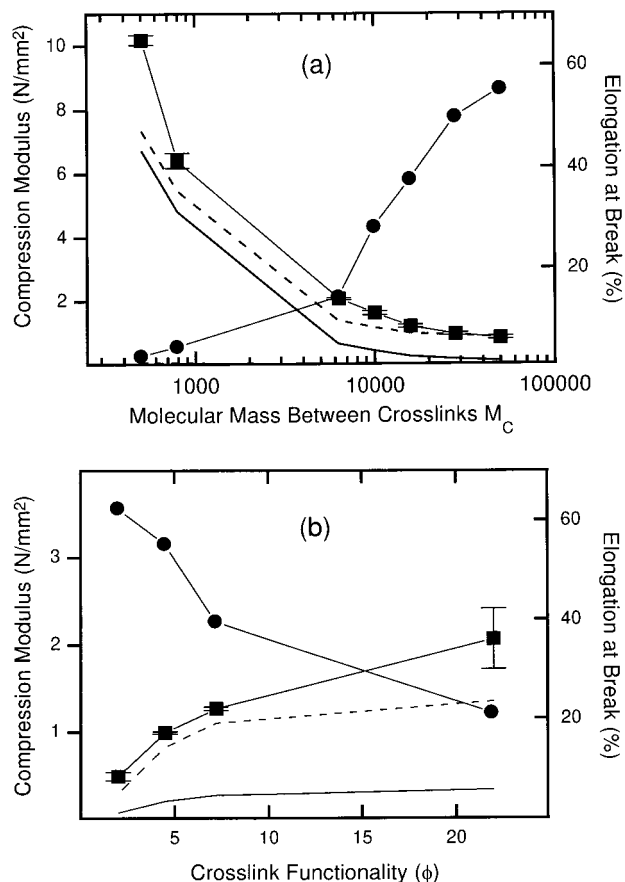

Figure 1. Modulus and elongation at break of model polymer networks as a function of (a) M_c and (b) ϕ. Calculated values of the modulus are plotted as (a) a solid line using the affine monomodal model and a dashed line using the affine bimodal model and (b) a solid line using the phantom monomodal model and a dotted line using the phantom bimodal model.

Thermal expansivity causes a linear shrinkage of the material upon cooling on the order of 1.5% for cures at 60 °C. The modulus and surface hardness were optimal for a resin-to-cross-linker ratio (*r*) of 10:1 (w/w) and decreased as the amount of cross-linker was increased or decreased. Longer curing times and higher temperatures allow at most a doubling of the modulus and hardness of the polymer. The reason for this increase is not clear, but we speculate that diffusion at higher temperatures improves the accessibility of vinyl groups for network-forming reactions. As Sylgard 184 is already filled with silica nanoparticles, we concluded that useful high-modulus stamp materials have to be formulated using higher cross-linked polymers.

We experimentally studied the dependence of surface hardness, compression modulus, and strain at break as a function of M_c from 550 to 49 500 D (Figure 1a)[27] using a short cross-linker ($\phi = 7.4$; 1050 D; 52.5% hydrosilane at the optimal hydrosilane-to-vinyl ratio). The calculated moduli were obtained using affine models with monomodal[28,29] and bimodal behavior.[29,30] In a second set of experiments (Figure 1b),[27] surface hardness, compression modulus, and strain at break were measured at variable ϕ (2−23) and constant M_c. The calculated moduli were obtained using phantom models with monomodal and bimodal[29] behavior. As model calculations predict, F^* decreases with increasing M_c (Figure 1a) and, less pronounced, with decreasing ϕ (Figure 1b).

The affine models underestimate the modulus even when the fraction of effective chains in the network (ν)

is set to 1. The difference between theory and experiment is 2-fold in the low-molecular-weight regime and nearly 10-fold for long chains with an almost constant absolute difference over the entire molecular weight range. The model predicts that the ratio of the molecular weights of the shortest and the longest molecular mass between cross-links is linearly reflected in the resulting modulus. This was not observed: we find that the modulus scales by a factor of ~12 instead of the predicted factor of 63. The prediction of moduli of our model materials with variable M_c using bimodal networks was more accurate.

Introduction of a constant factor of 5/3 (ref 30) improved the prediction of short-chain networks but still left a substantial difference in the long-chain case. If we assume that the short hydrosilane cross-linker (M_{c_2} = 1950 D) contributes equally as a second mode to the network, we can predict the appropriate difference between the shortest and longest chains in our study and give reasonably accurate absolute numbers.

The phantom model was used to predict moduli as a function of cross-linker functionality. The calculated moduli using monomodal behavior were much lower than the experimentally observed values, and again the use of bimodal calculations improved the accuracy. Mechanical parameters of the networks depend on the junction functionality at low values of ϕ; at higher values ($\phi > 3$) the dependency of the networks on this parameter is very small. The measured surface hardness was found to be linearly related to the modulus; no attempts have been made to calculate surface hardness, however. Experimentally, the surface hardness varied from 0.28 to 1.7% for M_c decreasing from 49 500 to 550 D (Figure 1a) and from 0.21% to 0.43% for ϕ increasing from 2 to 23 (Figure 1b). To the first order, elongation at break is inversely proportional to the modulus. Attempts to define models for strain at break using simple linear relationships that predict absolute numbers for toughness were not successful.

The results presented in Figure 1 demonstrate that we are able to formulate polymers with a high modulus but not yet with sufficient toughness (elongation at break >3%), an important feature of a useful stamp material. Reduced toughness leads to a brittle material that cannot be peeled off a master without fracturing. We therefore tested other material combinations having similar M_c and ϕ values but with vinyl copolymers instead of end-functional vinyl compounds. This approach resulted in materials having a surface hardness of up to 2.6% of glass and compression moduli on the order of 9 N mm^{-2} (Table 2). We obtained harder materials when M_c was reduced, i.e., when the fraction of functional group to dimethyl was higher (vinyl to dimethyl 1%, M_c = 7400 D up to 12%, M_c = 512 D) or ϕ was higher (hydrosilane to dimethyl between 6.5%, ϕ = 2 up to 52.5%, ϕ = 7.4). We did not include prepolymers with higher vinyl content because initial tests showed they do not polymerize well. Generally, the fraction of reactive sites had to be limited because of otherwise vigorous exothermic gas-generating side reactions that cause foaming or significant shrinkage. Optimal materials properties were found for a mixture having M_c = 987 D and ϕ = 7.2 (VDT-731, HMS-301). We preferred the softer mixture containing HMS-301 over the one containing HMS-501 because the latter had a greater tendency toward side reactions. The toughness of this material (elongation at break 5.7%) is at least

twice that of a material of similar hardness (DMS-V05) in Figure 1.

Bimodal materials were created and tested by adding 10–30% short-chain cross-linker (VMM-010) to end-functionalized chains (DMS-V22) and to vinylmethyl copolymers (VDT-731). The hydrosilane-to-vinyl ratio in these experiments was kept constant by adding an appropriate amount of the hydrosilane component already present (either HMS-301 or HMS-501). In the former case the modulus was improved at a relatively good toughness but not to a level better than VDT-731. These materials apparently already behave like bimodal systems, and the further addition of short chains cannot change this to a great extent. Calculations using the model of Flory[7] predict a modulus of 6.75 N mm^{-2} for a uniform monomodal network (VDT-731/HMS-301, M_c = 987 D, ϕ = 7.2). Taking the short cross-linker as a second mode with M_c = 266 and the appropriate volume fraction, one can predict a modulus of 11.1 N mm^{-2}. Predictions using the affine model of Sharaf and Mark[28] result in a modulus of 3.5 N mm^{-2} for the monomodal theory and 7.5 N mm^{-2} for the bimodal theory, thus confirming their bimodal nature.

Another parameter space that was explored with these polymers was filling with nanophase fillers to improve their modulus and toughness and to reduce volume shrinkage after polymerization. Two different types of fillers were used: a PDMS-based nanophase filler that was dispersed in another vinyl-functionalized prepolymer and can be linked into the polymer network via surface vinyl-functional groups and glass nanoparticles that are surface-modified to allow dispersion within a vinyl prepolymer: The PDMS-based filler did not improve the mechanical properties over those of the unfilled polymer, whereas addition of 5% (w/w) of the glass filler resulted in a compression modulus of 9.7 N mm^{-2}, a surface hardness of 3.3%, and a 1% reduction of the elongation at break.

Mixtures composed of 3.4 g of VDT-731 and 1.0 g of HMS-301 (material A) or additionally filled with 5% glass (material B) have a low viscosity in their precursor state, which facilitates accurate replication of the master structure. The high modulus of these polymers is optimal for replication of small structures but does not allow trimming or cutting without extensive cracking and generation of debris. The chemical and thermal shrinkage after cooling can cause the newly formed stamp to "snap" off the master and leads to distorted or ruptured structures; release of stamps from the master at higher temperatures can reduce this problem, however. Light scattering due to self-aggregation of the glass filler causes an opaque appearance of material B and could not be eliminated even by prolonged vigorous stirring (potter Evelhjem). The work of adhesion of both materials is on the order of 3 × 10^{-8} J mm^{-2} (compared to 1 × 10^{-7} J mm^{-2} for Sylgard 184), which is sufficient to form and maintain intimate contact with a flat substrate.

Comparison of the stress−strain curves in Figure 2 shows a strong trend toward embrittlement as M_c is reduced. Basically, the fracture energy for a given material should not depend on M_c, but experimentally a reduction of the fracture energy by a factor of 12 is observed as M_c is reduced from 9400 to 550 D. This is a common observation in monomodal PDMS materials and precludes the use of such materials as stamps. Hard bimodal materials, on the other hand, show a higher
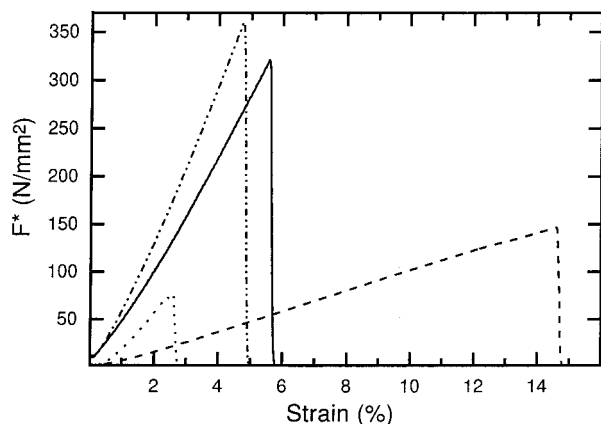
Figure 2. Stress–strain curves of representative siloxane networks. Monomodal networks ($M_c = 9400$, dashed line) show a reduction of fracture energy (integral below curve) as M_c is reduced and the material becomes harder ($M_c = 550$, dotted line). Bimodal materials ($M_{c_1} = 987$, $M_{c_2} = 266$, solid line; 5% silica filled, dashed–dotted line) show a substantial increase in fracture energy over the hard monomodal counterpart.

fracture energy and allow the use of harder polymers as stamps. Our design effort identified two polymers (A and B), which we subjected to pattern replication and pattern transfer tests. The advantages of these materials are illustrated in Figure 3. Whereas the commercial material (Sylgard 184), Figure 3a, is unsuitable for replication of patterns below 250 nm (indicated by the loss of feature definition in all but one of the quadrants), material B continues to allow the definition of useful reliefs down to 80 nm with an aspect ratio (depth/width of pattern) of 1.25 (Figure 3b). The paired posts (Figure 3b, lower left) stick to each other because deformations during stamp manipulation (demolding, inking, and printing) have brought them into contact from which they cannot snap back because of adhesion forces. In addition to the replication of small features, materials A and B allow features to be printed that have a lower density than is possible with Sylgard 184; i.e., useful aspect ratios can be varied over a wider range (from 5 down to 0.02). Selective surface hardening by in situ filling with TEOS[31,32] was not successful because the low-molecular-weight monomer swelled the preformed network hundreds of micrometers deep and severely distorted the overall stamp geometry.

The pattern replicated on a target surface by employing a "soft" stamp can suffer from geometric distortion during the various process steps. The origin and size of distortions are assessed for different stamp polymers and implementations. For a description of accuracy we have to identify a systematic (compensable) distortion between the master and the replicated stamp and random variations among successive prints from the same stamp. The latter is critical because it shows the intrinsic limitation of the reproducibility caused by (a) local mechanical instabilities of the structures, such as bending or collapsing, (b) nonuniform long-range distortions caused by mechanical forces during handling of the stamp, or (c) runout due to thermal fluctuations or solvent uptake during inking.

Rogers et al.[21] quantified long-range distortions using an elegant Moiré technique for soft elastomer stamps and stamps with rigid glass backplanes. Two printed patterns made with a stamp having a 0.1 mm thick elastomer layer on a rigid backplane were accurate to within 1 μm in an area of 1 cm^2.[21] Folch et al.[20] measured the deviation of a printed pattern from a reference pattern using a 4 in. stamp with a rigid backplane and found distortions of less than 5 μm. Structures cast with Sylgard 184 cannot be used for an accurate transfer of features smaller than 0.5 μm and having an aspect ratio of 1. For materials A and B, local deformations remain small down to pattern sizes of 100 nm and aspect ratios of 1. We extended these investigations to large-area stamps using the new polymers and concepts discussed above.

Unsupported stamps made of Sylgard 184 showed nonuniform pattern displacements up to 20 μm between two successive prints over areas of 5 × 5 cm^2. Prints of stamps made of material A or B were subjected to nonuniform distortion up to 30 μm over similar areas. We attribute the larger distortions of materials A and B to their greater temperature sensitivity and the need to press the rim of the stamp down manually to achieve conformal contact over the entire area. The thermal expansion coefficients of the stamps used were ∼260, ∼450, and ∼410 μm m^{-1} °C^{-1} for Sylgard 184, material A, and material B, respectively.

To reduce the long-range distortion, we tested several multilayer schemes using a glass or quartz backplane hybridized directly to the stamp polymer (Figure 4). The first system tested was a 90 mm diameter, 1 mm thick Sylgard 184 slab molded directly onto a 2.39 mm (0.9 in.) quartz plate (Figure 4c). With this stamp the maximal pattern distortions between two prints de-
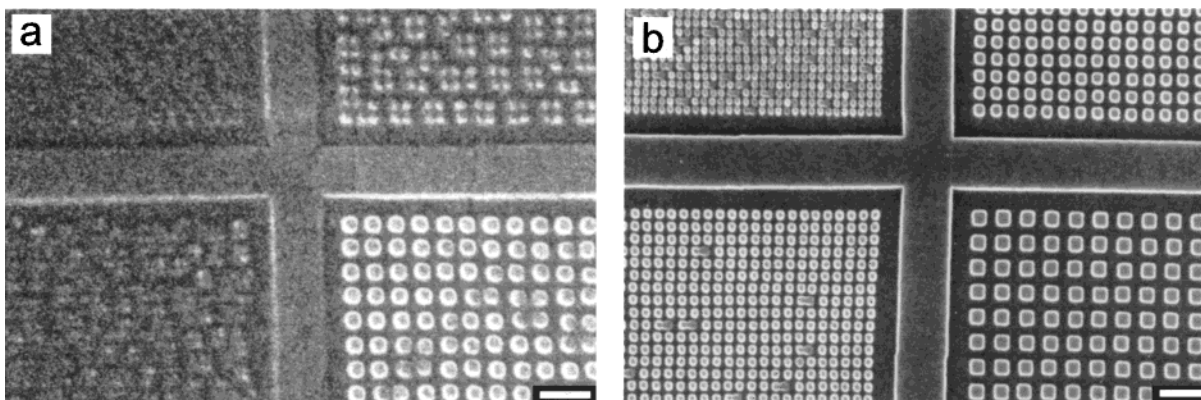

Figure 3. Comparison of high-resolution pattern replication by (a) Sylgard 184 with a compression modulus of 2 N/mm^2 and (b) material B with a compression modulus of 9.7 N/mm^2, bar = 1 μm. Squares of 250 × 250 nm^2 (lower right quadrant) already appear rounded in the Sylgard 184 stamp and are not stable enough for contact printing. Material B accurately replicates structures down to 80 nm (upper left quadrant). The height of the structures is 100 nm in both cases.
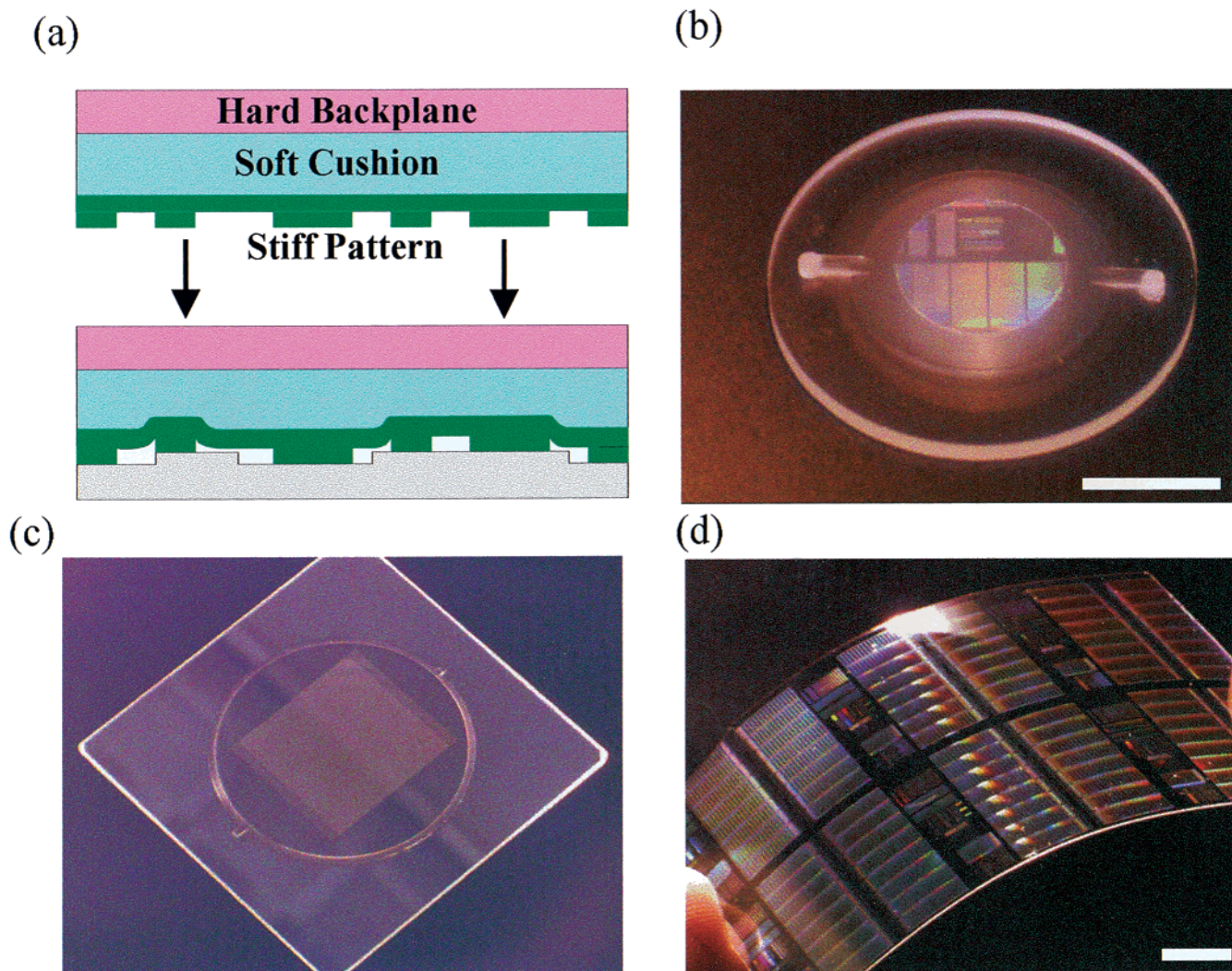
Figure 4. Examples of stamps. (a) Scheme of a trilayer stamp (glass backplane, elastomeric cushion, hard polymer, upper part) and a trilayer stamp in contact with an uneven substrate illustrating improved adaptivity (lower part). (b) Trilayer stamp with 270 nm features, bar = 10 mm. (c) Stamp 1 mm thick having >5 μm patterns molded in a soft siloxane polymer on a 125 mm glass plate. (d) Example of a two-layer thin film stamp composed of a 100 μm glass backplane and a 30 μm thick film of material B with 270 nm features, bar = 10 mm.

creased to ~1.5 μm over the entire area. We attributed the remaining distortion to the ability of the 1 mm thick elastomer layer to deform nonuniformly during contact. When a rigid quartz plate is used as backplane, the polymer material has to provide the elasticity to compensate for the substrate unevenness. Because polymers for high-resolution patterns have only a very limited elasticity, it is difficult to achieve contact over large areas in this implementation. With a 30 μm thick polymer layer of material B on an elastomeric cushion consisting of a 1 mm thick Sylgard 184 layer attached to a quartz plate (Figure 4a,b), the requirements concerning substrate flatness are relaxed and a layer of high-modulus polymer can conform readily to the substrate and transfer its pattern. The soft cushion is first molded on the quartz backplane. The resulting stamp is then placed on a master, precoated with the second polymer layer, and cross-linked. Stamps with rigid backplanes print with sufficient accuracy for many applications and can fit into mask-aligner tools made for "hard" contact lithography. However, they have two severe drawbacks when large printing areas are required. First, trapped air can disrupt the propagation of the contact front, and second, the rigid backplane

hampers a sequential release between stamp and master or substrate, resulting in separation forces that are great enough to damage the stamp, the master, or the substrate.

The third approach uses thin, flexible glass backplanes (Figure 4d) consisting of a 100 μm thick glass foil (Schott/DESAG, AF 45, 5 × 5 cm²) coated with a 75 μm thick structured (feature dimension ≥3 μm) layer of Sylgard 184 or a 30 μm thick structured layer of material B (feature dimension ≥120 nm). In this approach, the pattern distortion was uniform and the runout between two prints in the first case was ~500 or 100 nm cm^{-1}. In the second case with the harder material, runout was only ~330 or 55 nm cm^{-1}. Stamps with flexible backplanes avoid the limitations of unsupported as well as rigid backplane stamps while sharing their advantages: flexible stamps can be gradually released from the mold during manufacturing or from the substrate after printing. This helps overcome the large adhesion forces, and the better control over the contact front prevents air from being trapped during printing. Flexible backplanes follow the substrate topologies and allow the use of thinner polymer layers, which minimizes distortion, or harder polymer layers

without compromising their adaptivity to form intimate contact. If transparency of the stamp is not required, the glass foil can be replaced by a thin metal foil, which is less fragile and easier to handle.

4. Discussion and Summary

Stamps are the key elements in high-resolution soft lithography because they carry the pattern on their surface and are capable of conformal contact during printing. Soft lithography requires adaptation of the stamp to a potentially uneven substrate, but collapse, deformation, and runout must be avoided simultaneously. In fact a careful balance between desired and undesired deformation has to be maintained. We conducted extensive studies of molding and printing using materials with uniform properties in all dimensions. The resulting optimal material is always a compromise between the different competing requirements of conformal contact and pattern stability. Materials A ($M_c = 987$ D, $\phi = 7.2$) and B (with additional glass filler) have been found to be a good compromise and have the capability of replicating small features at 100 nm over 5×5 cm^2 areas with submicrometer accuracy.

Our study of "model" compounds produced an improved experimental understanding of the modulus as a function of the main network parameters (M_c, ϕ, bimodal M_{c_2}, and filler). Moduli and especially toughness could not be predicted with sufficient accuracy for our application, so experimental formulation and testing of networks composed on the basis of intuition will remain an important part of our work. The polymers formulated using the "copolymer" approach assuming constant M_c (987D for VDT-731) can be predicted only inaccurately using the model of Flory and Rehner (experimental 9, theory 6.6 N mm^{-2}).[7] If the short cross-linker is taken as a second phase, a modulus of 11.1 N mm^{-2} is predicted. A comparison between the model and experiments with the copolymer materials suggest that they behave like bimodal networks, although the exact chemical nature of the second mode is not entirely clear. The limitations in modulus and toughness found in networks from end-functionalized prepolymers were overcome by the use of copolymers as network elements. Another advantage of our new polymers is the higher chance of the multifunctionalized prepolymers (>7 vinyl groups per chain) to be linked into the network compared to end-functionalized prepolymers (2 vinyl groups per chain only). Sol fractions were 4.7% and 4.5% for the reference material and material A, respectively. Analysis of the prepolymers and the material extracted from the network showed the same amounts of low molecular cyclics. Extraction of the impurities on the level of the prepolymers would allow fabrication of polymers with reduced amounts of extractables in the future.

How materials properties change in the surface region is an additional issue of interest as the desired feature scale goes below 100 nm, because at these scales the modulus and other parameters of a polymer are no longer necessarily independent of feature sizes. Qualitative results demonstrate that the modulus of polymers at the surface is higher, probably because of the smaller number of possible chain configurations and the thereby created entropy effect.[33] With ever smaller dimensions of the stamp patterns, surface effects are bound to become increasingly important and will have to be addressed thoroughly in future studies.

Using the new stamp materials, high-resolution patterns of inks were printed in a classical microcontact-printing scheme.[34] The materials were also successfully used to transfer functional biological molecules[35] and to make a patterned contact to a resist in elastomeric light couplers.[36] These experimental results obtained with high-resolution stamps demonstrate the utility of the new polymers and allow the resolution limits of the various contact-printing methods to be assessed in a more direct way. We have addressed the issues of accuracy and overlay using our hybrid stamps: Long-distance accuracy or runout has been reduced to levels below 500 nm over a distance of 5 cm. Overlay accuracies have been determined to be on the order of 1 μm over the same areas.

We have seen that several requirements of lithography can be met using the newly developed materials and the hybrid-stamp concept. One important problem remains with all thermocured materials: Polymers shrink upon cooling and create residual stresses in the stamp. Stresses are not a severe problem in very thin hybrid stamps, but a stress-free system is clearly desirable. Possible solutions to the thermal-stress problem are ultraviolet-curable systems or thermocured systems that cure at room temperature. Both approaches have disadvantages, which will have to be addressed in future studies: ultraviolet-curable systems have a high fraction of extractables, including the added radical initiators, and require more expensive prepolymers. Room-temperature cure materials are generally softer, have a higher fraction of extractables, and require much longer curing times than their high-temperature cure counterparts. Generally, hard polymers are very brittle and more difficult to handle than softer materials. Additional pendant groups of mixed copolymers might help improve this characteristic by having greater toughness than that of similar pure dimethylsiloxanes. Pendant groups might also be helpful for changing the surface properties of stamps, for allowing the direct printing of hydrophilic inks or molecules without harsh surface treatments, or for acting as anchors to graft other polymers. Finally, chemical treatments of the stamp surface can be used to create surface functional groups or to harden top layers by in situ filling, for example, refs 31 and 32. The improvements of resolution and accuracy as a consequence of the better stamp materials and hybrid stamp designs as well as the potential for their further optimization mentioned above show that work in this area will continue to be crucial to the success of soft lithography.

References and Notes

(1) Johnson, T. *Proceedings of the 152nd ACS Rubber Division Meeting*, Cleveland, OH, 1997; Vol. 30, p 11.
(2) Wong, C. P. *IEEE Trans. Comput. Packag. Manuf. Technol., A* **1995**, *18*, 270.

(3) Kardos, J. L.; Gadkaree, K. P.; Bhate, A. P.; Chiellini, E.; Giusti, P.; Migliaresi, C.; Nicolais, L. *Polym. Sci. Technol.* **1986**, *34*, 187.

(4) Xia, Y.; Whitesides, G. M. *Angew. Chem., Int. Ed.* **1998**, *37*, 550.

(5) Sharaf, M. A.; Mark, J. E. *Polymer* **1994**, *35*, 740.

(6) Rennar, N.; Oppermann, W. *Colloid Polym. Sci.* **1992**, *270*, 527.

(7) Flory, P. J.; Rehner, J. *J. Chem. Phys.* **1943**, *11*, 512.

(8) Mark, J. E. *Acc. Chem. Res.* **1985**, *18*, 202.

(9) Dusek, K.; Prins, W. *Adv. Polym. Sci.* **1969**, *6*, 1.

(10) Flory, P. J. *Macromolecules* **1982**, *15*, 99.

(11) Flory, P. J.; Erman, B. *Macromolecules* **1982**, *15*, 800.

(12) Mark, J. E.; Erman, B. *Rubberlike Elasticity: A Molecular Primer*; Wiley: New York, 1988.

(13) Flory, P. J. *J. Polym. Sci.* **1984**, *22*, 49.

(14) James, H. M.; Guth, E. *J. Chem. Phys.* **1947**, *15*, 669.

(15) Wang, S.; Mark, J. E. *J. Polym. Sci., B* **1992**, *30*, 801.

(16) Visser, S. A. *J. Appl. Polym. Sci.* **1997**, *63*, 1805.

(17) Delamarche, E.; Schmid, H.; Michel, B.; Biebuyck, H. *Adv. Mater.* **1997**, *9*, 741.

(18) Biebuyck, H. A.; Michel, B. WO 97/06012, 1997.

(19) Biebuyck, H. A.; Larsen, N. B.; Delamarche, E.; Michel, B. *IBM J. Res. Dev.* **1997**, *41*, 159.

(20) Folch, A.; Schmidt, M. A. *J. Microelectromech. Syst.* **1999**, *8*, 85.

(21) Rogers, J. A.; Paul, K. E.; Whitesides, G. M. *J. Vac. Sci. Technol., B* **1998**, *16*, 88.

(22) Macosko, C. W.; Saam, J. C. *Polym. Bull.* **1987**, *18*, 463.

(23) Saechtling, H. *International Plastics Handbook*, 3rd ed.; Hanser: Munich, 1995.

(24) For more information about the surface hardness measurement see http://www.zurich.ibm.com/technologies/conprint/tools.

(25) Israelachvili, J. *J. Vac. Sci. Technol., A* **1992**, *10*, 2961.

(26) For more information about Sylgard 184 see http://www.zurich.ibm.com/technologies/conprint/sylgard.

(27) Tables for Figure 1 available at: http://www.zurich.ibm.com/technologies/conprint/table.

(28) Sharaf, M. A.; Mark, J. E.; Ahmed, E. *Colloid Polym. Sci.* **1995**, *272*, 504.

(29) Erman, B.; Mark, J. E. *Structures and Properties of Rubberlike Networks*; Oxford University Press: Oxford, 1997.

(30) Sharaf, M. A.; Mark, J. E. *J. Polym. Sci.* **1995**, *33*, 1151.

(31) Sur, G. S.; Mark, J. E. *Eur. Polym. J.* **1985**, *21*, 1051.

(32) Wen, J.; Mark, J. E. *Rubber Chem. Technol.* **1994**, *67*, 806.

(33) Wang, P.; Guo, J.; Wunder, S. L. *J. Polym. Sci., B* **1997**, *35*, 2391.

(34) Delamarche, E.; Schmid, H.; Bietsch, A.; Larsen, N. B.; Rothuizen, H.; Michel, B.; Biebuyck, H. A. *J. Phys. Chem.* **1998**, *102*, 3324.

(35) Bernard, A.; Delamarche, E.; Schmid, H.; Michel, B.; Bosshard, H. R.; Biebuyck, H. *Langmuir* **1998**, *14*, 2225.

(36) Schmid, H.; Biebuyck, H.; Michel, B. *Appl. Phys. Lett.* **1998**, *72*, 2379.

MA982034L